

---

# Metabolism of Indium-111-Labeled Murine Monoclonal Antibody in Tumor and Normal Tissue of the Athymic Mouse

Cecilia Motta-Hennessy, Robert M. Sharkey, and David M. Goldenberg

*Center for Molecular Medicine and Immunology, University of Medicine and Dentistry of New Jersey, Newark, New Jersey*

---

We have studied the fate of radiometal metabolism *in vivo* by analyzing the molecular form of radiolabeled anti-carcinoembryonic antigen (CEA) in tissues. Athymic mice bearing colonic tumor xenografts were injected *i.v.* with  $^{111}\text{In}$ -isothiocyanate-benzyl-DTPA-(SCN-Bz-DTPA) IgG or  $^{111}\text{In}$ -(SCN-Bz-DTPA) F(ab')<sub>2</sub>, and then killed daily for up to four days. Liver, kidney, and tumor were extracted and the supernatants, plasma and urine samples were analyzed by HPLC, ITLC, HPIEC and SDS-PAGE. By HPLC, the activity in normal tissue and tumor was associated principally with two major components. The first was native MAb and the second was a low molecular weight component (LMWF). On Day 1, the native-sized IgG was the predominant form (>65%), but progressively decreased to less than 20% by Day 4. For the F(ab')<sub>2</sub>, even by Day 1 ~90% of the activity was associated with the LMWF. This LMWF was resolved further by HPIEC and SDS-PAGE into several metabolites that appear to be  $^{111}\text{In}$ -SCN-Bz-DTPA and  $^{111}\text{In}$ -SCN-Bz-DTPA bound to peptide fragments.

**J Nucl Med 1990; 31:1510-1519**

---

**R**adiolabeled antibodies against antigens associated with human tumors are being evaluated extensively for tumor imaging and therapy (1-3). Initially, radioisotopes of iodine, principally iodine-131 ( $^{131}\text{I}$ ) were used for labeling, but more recently, indium-111 ( $^{111}\text{In}$ ) has been used for this purpose (4,5). These techniques involve the use of bifunctional chelates (BC), molecules that can be attached covalently to an antibody, but can still retain their capacity to bind metal ions (6). Some of the most commonly used BC are derivatives of EDTA or DTPA (7,8). Many chemical reactions have been used to link chelating groups to proteins. The first step requires the modification of the chelate, either by formation of an anhydride (mixed anhydride or cyclic

anhydride) of DTPA (9) or by attachment of a reactive group to one of the nitrogen atoms (10). Reaction of the modified chelate with the antibody results in covalent attachment of the chelate, usually to the epsilon-amino group of lysine. Covalent linking offers the possibility of stronger bonding between the antibody and the radionuclide, than the electrophilic bonding of radioiodine. Nevertheless, slow release of the radiometal from the antibody conjugate is thought to produce a continuous leakage of the radionuclide into the blood, resulting in radiometal transport to normal tissue, particularly liver and bone (11). Accretion of  $^{111}\text{In}$ -labeled-MAb interferes with the detection of tumor metastasis in the liver (12). A reduction in accretion in the bone is of major importance, especially if radiolabeled antibodies are to be used for tumor therapy with beta emitters, such as yttrium-90 ( $^{90}\text{Y}$ ), due to its bone marrow toxicity (13). Such concerns have led several investigators to design stronger chelates for binding radiometals (14), and to search for more specific antibody modification by attaching DTPA chelates to the immunoglobulin carbohydrate (15), or by introducing a metabolizable linkage between the metal chelate and antibody (16). Although many of these attempts have produced better radiometal-antibody conjugates and have, in some cases, reduced liver and bone uptake moderately (17,18), the nature of this liver and bone marrow accretion is not fully understood.

In this paper, we have investigated the metabolism of  $^{111}\text{In}$ -(SCN-Bz-DTPA)-anti-CEA MAb IgG and its F(ab')<sub>2</sub> fragment in normal tissue and xenografted tumor, including the rate of catabolic breakdown of the material and the molecular forms of the radiometal in plasma, liver, kidney, and urine after *i.v.* administration.

## MATERIALS AND METHODS

### Preparation and Conjugation of anti-CEA IgG and Its F(ab')<sub>2</sub> Fragment

The murine anti-CEA MAb designated NP-4 (19) was isolated from mouse ascites by Protein A and ion exchange chromatography, and its purity checked by immunoelectro-

---

Received Nov. 3, 1989; revision accepted Mar. 6, 1990.  
For reprints contact: David M. Goldenberg, ScD, MD, Center for Molecular Medicine and Immunology, 1 Bruce St., Newark, NJ 07103.

phoresis, SDS-PAGE, and isoelectric focusing. F(ab')<sub>2</sub> was prepared by pepsin digestion and isolated from the peptide fragments by Q-Sepharose (Pharmacia, Piscataway, NJ). The isothiocyanate benzyl-DTPA (SCN-Bz-DTPA) conjugate was obtained from Immunomedics, Inc. (Newark, NJ). It was conjugated by adding the antibody (5.0 mg/ml) previously dialyzed against 100 mM Hepes buffer, pH 8.6, containing 150 mM NaCl, at a 8:1 molar excess of DTPA to MAb. After overnight incubation at room temperature, the MAb-conjugate was purified from unreacted SCN-Bz-DTPA by gel filtration chromatography using a 25 × 1 cm Sephadex G-50 column (Pharmacia) that was demetalized by washing with 300 ml 50 mM DTPA, and equilibrated with 300 ml metal-free 20 mM MES (2[N-morpholino] ethanesulfonic acid) buffer, pH 6.0. All materials used in the preparation of the conjugate and during radiolabeling were rendered metal-free by acid-washing with 2.0 M HCl. Buffers were prepared using metal-free water and were passed over a column packed with Chelex (Bio-Rad, Richmond, CA). Fractions from the G-50 column containing MAb-chelate conjugate were collected and concentrated, using a Centricon miniconcentrator (Amicon, Danvers, MA), to 20 mg/ml and stored in acid-washed Eppendorf tubes at 4°C. The conjugates were determined to have between 1-2 DTPA per MAb molecule by quantification of cobalt-57 binding, as described previously (20).

### Radiolabeling of MAb-Conjugate

Indium-111-chloride (Nordion International, Ontario, Canada) was converted to <sup>111</sup>In-citrate by addition of two volumes of 1% citric acid, pH 4.0, and the MAb-conjugate was added at a ratio of 1.0 mg MAb to 5.0 mCi (185 MBq) of <sup>111</sup>In-citrate and incubated for 1 hr at room temperature. The labeling was monitored using silica gel chromatography (ITLC) developed with 1% citrate:methanol, pH 4.0. Prior to final purification, the labeled preparation was challenged with 5 μl 100 mM EDTA, and the (instant thin-layer chromatography) ITLC assay was repeated. For most experiments, the labeled antibody was separated from unbound <sup>111</sup>In-citrate by passage through an AvidChrome cartridge (Bioprobe International, Tustin, CA) equilibrated in 20 mM MES buffer, pH 6.0, 150 mM NaCl. However, for one study the unbound indium was not separated from the labeled MAb after EDTA challenge. The specific activity of the labeled antibody was 4–5 μCi/μg. Quality control was conducted on each antibody preparation. The immunoreactivity of the radiolabeled conjugate was determined by passage over a CEA immunoabsorbent prepared from Affigel-10 (Bio-Rad, Richmond, CA) and CEA extracted from the GW-39 human colonic tumor (21). Nonspecific binding was evaluated by passage over an AFP-immunoabsorbent. The percentage of activity in the adsorbed fractions was related to the total activity recovered. Each labeled preparation was also analyzed by high-performance liquid chromatography (HPLC) (Zorbax GF-250, DuPont, Willmington, DE) for determination of radioactivity associated with native size IgG or F(ab')<sub>2</sub>, or traces of unbound <sup>111</sup>In. The MAb-conjugate was monitored using an in-line UV monitor and radiation detector.

### Animal Studies

Female athymic mice (nu/nu; Harlan, Madison, WI) at 4–5 wk of age (15.0–18.0 g) were injected subcutaneously with 0.2 ml of a 10% suspension of the CEA-producing human

colonic tumor xenograft, GW-39 (22), that is serially propagated in nude mice. Two weeks later, when the tumor size was 0.15–0.25 g, the animals (n = 5 for IgG; n = 3 for its F(ab')<sub>2</sub> fragment) were injected intravenously with 1.0–5.0 mCi <sup>111</sup>In-SCN-Bz-DTPA-NP-4 IgG or its F(ab')<sub>2</sub> fragment and sacrificed 1, 2, 3, or 4 days later. Liver and kidney were treated in three steps: (1) perfused in situ with 1 ml cold 0.1 M Tris-citrate buffer, pH 6.5, containing 0.15 M NaCl, 0.02% sodium azide, 4.0 mg/ml aprotonin, 2 mM phenylmethylsulfonyl fluoride, 2 mM benzamidine-HCl, and 2 mM iodoacetamide to reduce possible in vitro degradation; (2) excised and placed in plastic tubes for determination of activity in a dose calibrator and frozen at –70°C; (3) thawed and homogenized by cell disruption using a Brinkman polytron at full speed for three, 30-sec bursts. The homogenization of the tissues was performed on ice using 2–7 ml of the buffer containing 35 mM beta-octyl-glucoside. The tumor tissue was treated in the same way as explained above but was not perfused. These preparations were centrifuged at 48,000 × g for 20 min in a Sorval-RC-5 centrifuge (Du Pont Instruments, Wilmington, DE). This process sediments nuclei, large plasma membrane sheets, unbroken cells, mitochondria and intact lysosomes. The supernatants and pellets were separated and counted in a dose calibrator. Supernatants as well as plasma and urine samples were filtered through a 0.45-μm filter (Acro LC 13, Gelman, Ann Arbor, MI) and analyzed by size-exclusion HPLC (Zorbax GF-250). The mobile phase at a flow rate of 1.0 ml/min was 50 mM sodium citrate, 150 mM NaCl, and 0.02% sodium azide, pH 6.5. The percentage of radioactivity in each peak was detected with a Beckman radioactivity monitor (Model 170) interfaced with an IBM-AT computer. Supernatants of tissue samples from animals sacrificed 24 hr postinjection were passed through a Sephadex G-50 column (35 × 1.0 cm) equilibrated and eluted with 20 mM Tris-buffer, pH 7.0. The antibody peak was recovered near the void volume of the column (tubes 6–15) and a second low molecular weight fraction (LMWF, tubes 21–36) was isolated and further analyzed by ITLC, SDS-PAGE and HPIEC.

### Controls

The stability of the radiolabeled IgG and F(ab')<sub>2</sub> fragment to the extraction procedure was tested by processing the radiolabeled MAb alone or in the presence of normal liver and kidney in an identical fashion as tissues recovered from animals injected with <sup>111</sup>In-labeled MAb. A group of three animals was also injected with <sup>111</sup>In-SCN-Bz-DTPA (5 mM DTPA, 1.0 mCi <sup>111</sup>In), and liver and kidney tissues as well as plasma and urine samples were processed and analyzed as described above.

### Thin-Layer Chromatographic Analysis (TLC)

TLC was performed using silica gel chromatography (SG) plates (Baker, Phillipsburg, NJ) with methanol: concentrated ammonia, 4:1 (v/v), pH 10.0, or with ITLC strips (Gelman, Ann Arbor, MI) with methanol: 1% citric acid, 1:1 (v/v), pH 4.0. TLC samples included the LMWF from the G-50 analysis of liver and kidney extracts, urine, and plasma (24-hr samples). <sup>111</sup>In-DTPA was included as a control. Five microliters of each sample were spotted at the origin and developed until the solvent migrated to the solvent front line. The plates were removed from the chamber and sprayed with 0.1% ninhydrin in methanol. They were then cut (ITLC strips) or scraped (SG

plates) in 1.0-cm sections, placed in individual vials, and assayed for radioactivity in a gamma counter.

### SDS-PAGE

The LMWF of the liver and kidney extracts was isolated by G-50 chromatography and analyzed on polyacrylamide gel electrophoresis using a 15% gel containing 8.0 M urea under denaturing conditions. Urine samples were also analyzed by SDS-PAGE. Low molecular weight carbon-14-methylated protein standards (Amersham, Arlington Heights, IL) were used as molecular weight markers. After running the gels at 150 V for 1.5 hr, they were either dried and analyzed by autoradiography using a X-Omat AR film (Kodak, Rochester, NY) or stained using 0.2% Coomassie blue (Bio-Rad, Richmond, CA), and dried for comparison to the unstained gels.

### High Pressure Ion Exchange Chromatography (HPIEC)

Analysis of the LMWF from the liver extract was also carried out using an HRLC-MA7P cartridge (Bio-Rad), a high capacity weak anion exchanger for peptide analysis. A gradient system for 20 mM Tris buffer, pH 8.5, with increasing NaCl concentrations at a flow rate of 1.0 ml/min and a pressure of 700 psi was used. Twenty microliter samples of liver extract (LMWF) and  $^{111}\text{In}$ -DTPA were loaded into the cartridge and the fractions were collected and analyzed for radioactivity in a gamma counter.

## RESULTS

### Radiolabeling of the MAb Conjugate, (SCN-Bz-DTPA)-NP-4, Its F(ab')<sub>2</sub> Fragment, and Quality Assurance

In all the experiments, the labeled NP-4 IgG or its F(ab')<sub>2</sub> fragment was recovered in the first 2.0-ml eluate from the AvidChrome cartridge, containing between 80–90% of the initial radioactivity for the IgG and between 77–80% for the fragment as determined by ITLC or HPLC. Between 80% to 90% of the  $^{111}\text{In}$ -labeled antibodies bound to the CEA-affinity column.

The binding to an irrelevant immunoadsorbent (AFP-Affigel) was only 3% to 5%. There was only 3% aggregation, as determined by size-exclusion HPLC, and no unbound  $^{111}\text{In}$  was found in the antibody preparation prior to injection.

### Animal studies

The amount of homogenization buffer used was important in extracting radioactivity from normal tissues and tumor efficiently. When the tissues were extracted using 2 ml of buffer, a ratio of 1.5:1 v/w for the largest organ (liver), only 40% of the initial activity was recovered in the supernatant and the rest remained in the pellet. However, more than 90% of the activity was extracted from normal tissue and tumor using 7.0 ml of buffer, a ratio of 5:1 v/w for liver. A good minimum ratio appears to be 5 ml of buffer to 1 g of tissue.

### HPLC Analysis of Tissue Extracts

Samples (20–500  $\mu\text{l}$ , according to the counts on the day of analysis) of tissue and tumor extracts were applied to the HPLC column. For the liver and kidney tissues, between 75%–87% of the applied activity was recovered from the column. In the case of tumor tissue, the recovered activity was between 68%–78%. The HPLC profiles depicted in figures 1–5 represent a percent of recovered activity from the column.

In the liver extract,  $^{111}\text{In}$ -NP-4 IgG was distributed between two major peaks. The first was native MAb, which decreased from 68% of the total activity in the extract on Day 1 to 2% by Day 4. The second was a LMWF that increased from 29% on Day 1 to 96% on Day 4 (Fig. 1). In the kidney, the conjugate was also distributed between two major peaks. The native MAb conjugate decreased from 85% of the total activity in the extract on Day 1 to 69% by Day 2. On Day 3 this native IgG peak was further metabolized to two minor

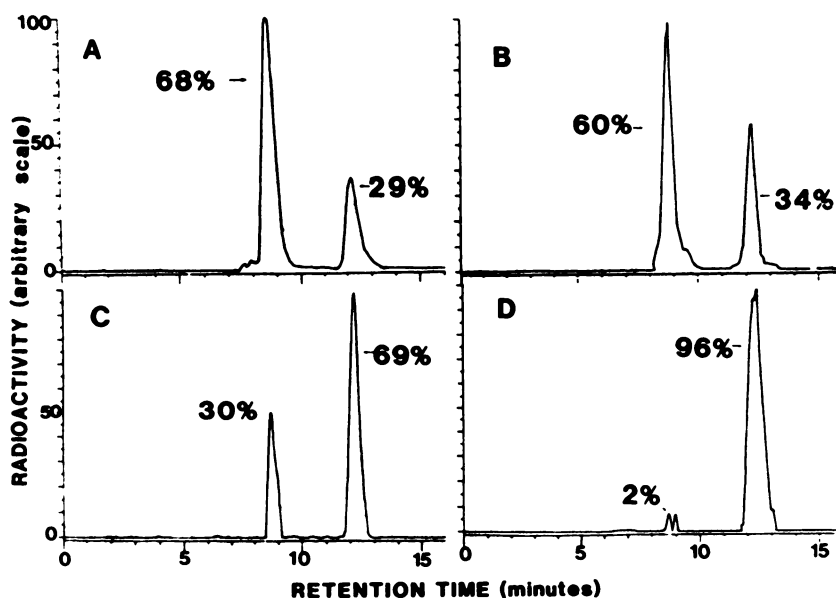


**FIGURE 1**  
Time-course study of catabolic breakdown of  $^{111}\text{In}$ -SCN-Bz-DTPA-NP-4 IgG in liver extract. (A) Day 1; (B) Day 2; (C) Day 3; and (D) Day 4.

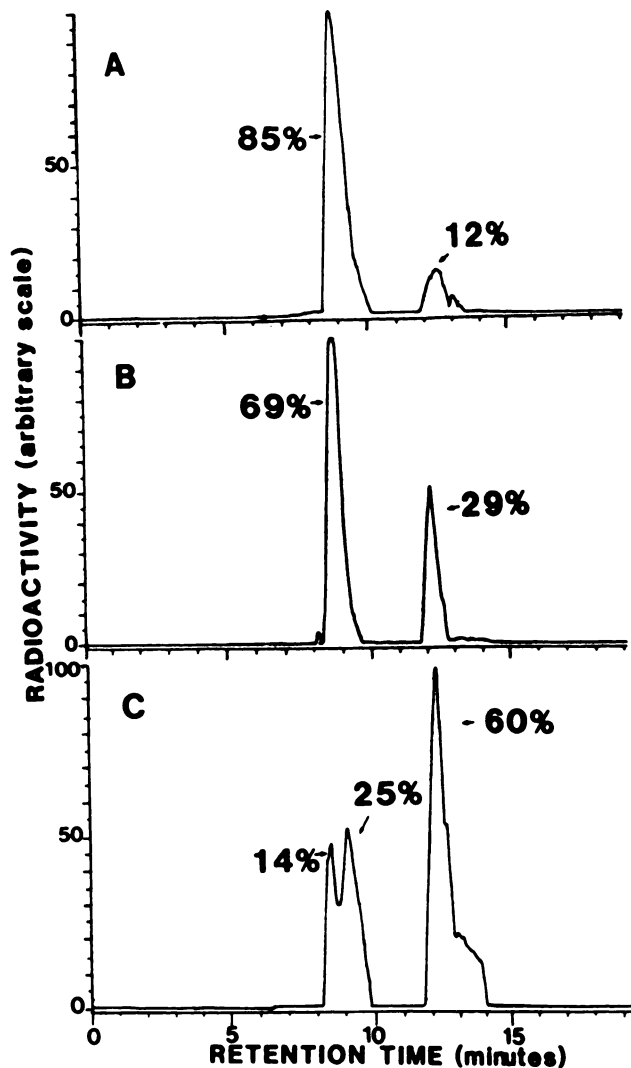


**FIGURE 2**  
Time-course study of catabolic breakdown of  $^{111}\text{In-SCN-Bz-DTPA-NP-4}$  IgG in kidney extract. (A) Day 1; (B) Day 2; and (C) Day 3.

peaks containing 14% and 25% of the radioactivity, suggesting some differences in the way the kidney processes the labeled antibody. The LMWF increased from 12% on Day 1 to 60% by Day 3 (last day analyzed for kidney), reflecting the rate of metabolic breakdown in these tissues (Fig. 2). In liver and kidney,  $^{111}\text{In-NP-4-F(ab')}_2$  fragment appeared to be metabolized more quickly than whole IgG. On Day 1 only 11% (liver) and 7% (kidney) of the radioactivity was associated with the native  $\text{F(ab')}_2$ , and on Day 2 all of the activity was recovered with the LMWF (Fig. 3). In Figure 3A, there is a small peak with a retention time (RT) of 9.7 and 5% of the recovered activity. This peak was not identified, but due to the RT of 9.7 for  $\text{Fab}'$  in this column, it could be  $\text{Fab}'$  fragments. It is presumed that the labeled NP-4 fragment may be processed in the liver with the formation of NP-4- $\text{Fab}'$ . In the same figure (Panel B), there is a second peak with a RT of 13.4 and 15% of the recovered activity. This peak is due to low molecular weight components that cannot be resolved further by this column. The native MAb or its fragment recovered in the liver, kidney and tumor extracts showed 80%–90% immunoreactivity by affinity column chromatography, whereas the LMWF in these tissues was not immunoreactive.

In the plasma, 100% of the activity was associated with the native MAb, either the NP-4 IgG or the fragment, and no measurable amount of unbound  $^{111}\text{In}$  was detected (Fig. 4). This suggests that the chelator remains firmly associated to the MAb in vivo, and that  $^{111}\text{In}$  does not suffer any considerable ligand exchange with plasma proteins. In the urine, most of the measured radioactivity was associated with the LMWF (Fig. 4). In the tumor, the radioactivity was recovered in three major peaks (Fig. 5). The first peak (retention time = 7.5 min) was not analyzed in detail, but due to

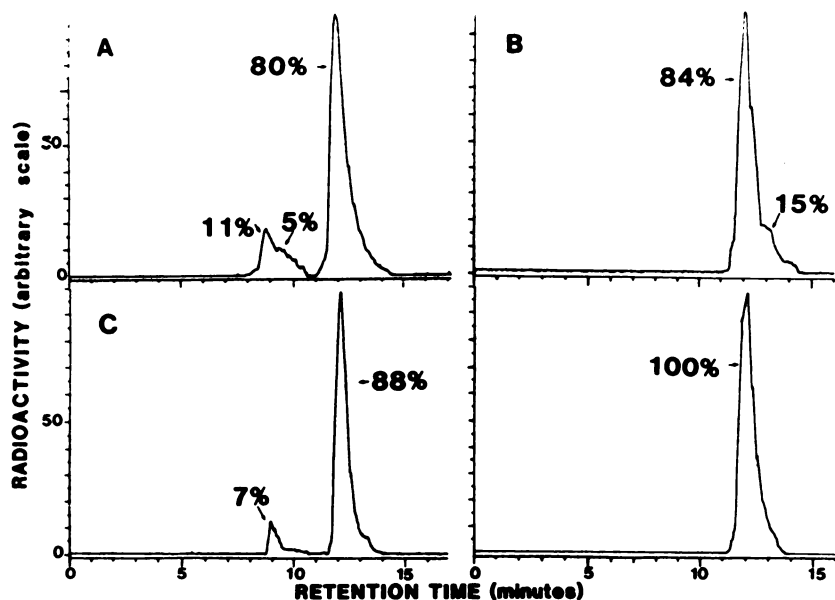
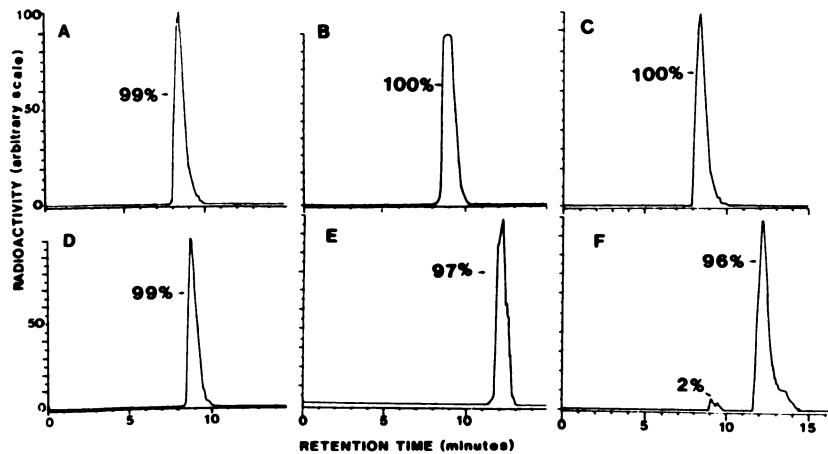


**FIGURE 3**  
Time-course study of catabolic breakdown of  $^{111}\text{In-SCN-Bz-DTPA-NP-4 F(ab')}_2$  in liver and kidney extracts. (Top) Liver: A = Day 1; B = Day 2; (Bottom) Kidney: C = Day 1; D = Day 2.

**FIGURE 4**  
Size-exclusion HPLC profiles of plasma and urine samples 1 to 4 days after i.v. injection of  $^{111}\text{In}$ -SCN-Bz-DTPA-NP-4 IgG and its  $\text{F}(\text{ab}')_2$  fragment. (Top) Plasma, IgG: A: Day 1; B: Day 2; C: Day 4. Bottom: D: Plasma,  $\text{F}(\text{ab}')_2$ , Day 1, E: urine,  $\text{F}(\text{ab}')_2$  Day 1; F: urine, IgG Day 1.



its large size it is presumed to be MAb-antigen complexes. The radioactivity in this peak decreased from 51% on Day 1 to 15% on Day 4. The second (retention time = 8.5 min) was native MAb that was 29% of the total activity on Day 1 and was undetectable by Day 4.

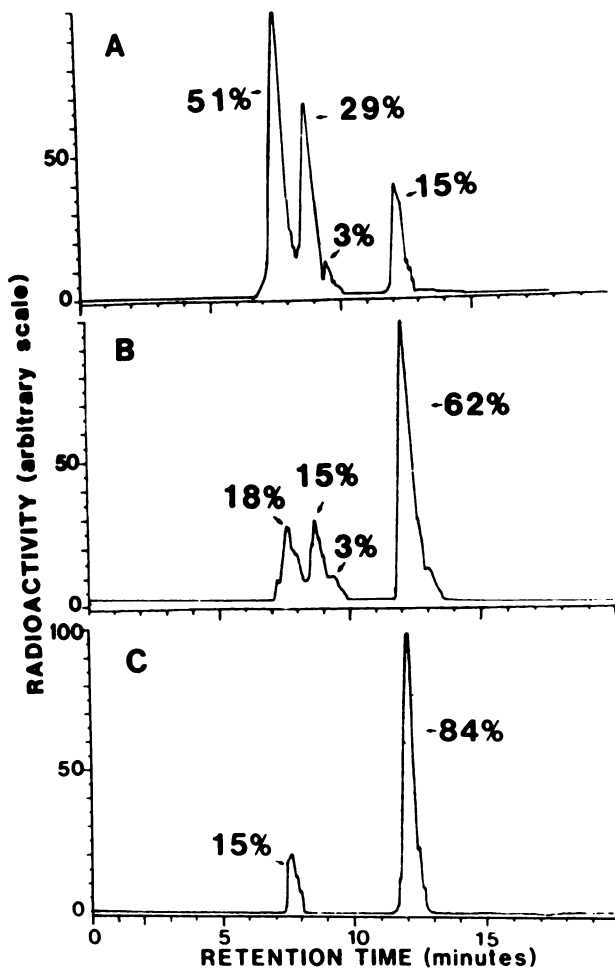


**FIGURE 5**  
Time-course study of catabolic breakdown of  $^{111}\text{In}$ -SCN-Bz-DTPA-NP-4 IgG in the GW-39 tumor. A: Day 1; B: Day 3; and C: Day 4.

The third was the LMWF that increased from 15% on Day 1 to 84% on Day 4. These results indicate that labeled MAb is catabolized at about the same rate in the tumor as in the normal tissues.

HPLC analysis of kidney and liver perfusates showed 100% of the activity associated with native IgG or native  $\text{F}(\text{ab}')_2$  fragment, suggesting that this activity is similar to that found in the plasma. Size exclusion HPLC analysis of control tissues and injected material showed that after the extraction procedure, the majority of the activity remained associated with the native MAb, suggesting that the methodology used did not alter the labeled MAb (results not shown).

In the liver and kidney extracts of animals injected with  $^{111}\text{In}$ -SCN-Bz-DTPA, all of the extractable radioactivity was present in the LMWF when analyzed by HPLC. Furthermore, when unbound  $^{111}\text{In}$  (25%) was not separated from the labeled MAb before injection, the percentage of radioactivity associated with the LMWF in liver and kidney extracts was not significantly different than when the  $^{111}\text{In}$ -labeled MAb was purified from this unbound material before injection (data not shown). This result suggests that the unreacted  $^{111}\text{In}$ , after EDTA challenge in the labeled preparation, was rapidly excreted, presumably as  $^{111}\text{In}$ -EDTA rather than being taken up by the liver.

**SDS-PAGE Analysis**

Figure 6 shows the analysis of the LMWF from liver and kidney extracts of mice injected with labeled IgG,  $\text{F}(\text{ab}')_2$ , or  $^{111}\text{In}$ -SCN-Bz-DTPA (control group). Most of the activity migrated to the bottom of the gel (lanes 2, 6 and 4, 8) in a similar fashion to  $^{111}\text{In}$ -SCN-Bz-DTPA (lane 1). Two to three additional  $^{111}\text{In}$ -labeled metabolites are present (MW 3,400–2,350) that may be  $^{111}\text{In}$ -SCN-Bz-DTPA associated with peptide fragments, since these bands of radioactivity stain with Coomassie blue (Fig. 7), whereas the fastest migrating band, presumed to be  $^{111}\text{In}$ -SCN-Bz-DTPA, did not stain with this protein detection reagent. These low molecular weight metabolites appear to be processed further in

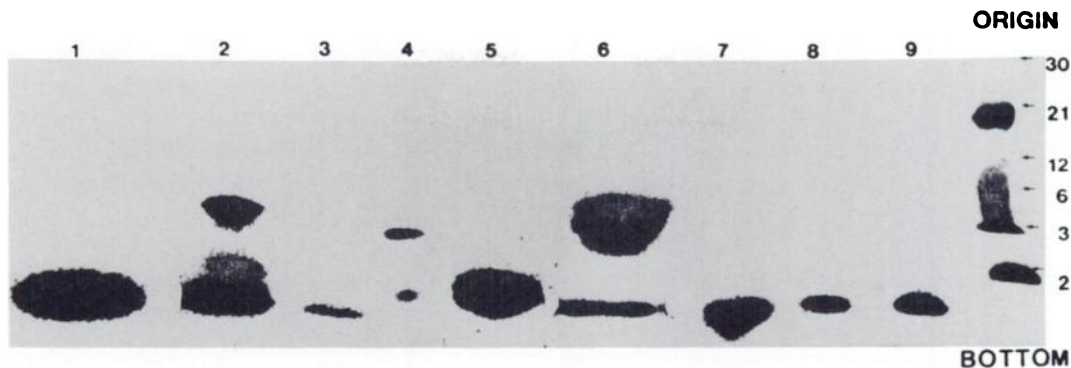


**FIGURE 6**  
 SDS-PAGE analysis (under reduction conditions) of  $^{111}\text{In}$ -SCN-Bz-DTPA-NP-4 IgG,  $\text{F(ab')}_2$  and  $^{111}\text{In}$ -DTPA in tissue extracts and urine 24 hr after injection: lane 1,  $^{111}\text{In}$ -DTPA; lane 2,  $^{111}\text{In}$ -SCN-Bz-DTPA-NP-4 IgG liver extract (LMWF); lane 3,  $^{111}\text{In}$ -SCN-Bz-DTPA-NP-4-IgG urine; lane 4,  $^{111}\text{In}$ -SCN-Bz-DTPA-NP-4  $\text{F(ab')}_2$  liver extract; lane 5,  $^{111}\text{In}$ -DTPA liver extract (LMWF); lane 6,  $^{111}\text{In}$ -SCN-Bz-DTPA-NP-4-IgG kidney extract (LMWF); lane 7,  $^{111}\text{In}$ -DTPA kidney extract (LMWF); lane 8,  $^{111}\text{In}$ -SCN-Bz-DTPA-NP-4  $\text{F(ab')}_2$  kidney extract; lane 9,  $^{111}\text{In}$ -SCN-Bz-DTPA-NP-4  $\text{F(ab')}_2$  urine; lane 10,  $^{14}\text{C}$ -labeled low molecular weight standards: carbonic anhydrase (30,000); trypsin inhibitor (21,500); cytochrome c (12,500); aprotinin (6,500); insulin (5,740). (After sample preparation, the insulin may break into the A (MW 2,350) and B chain (MW 3,400).)

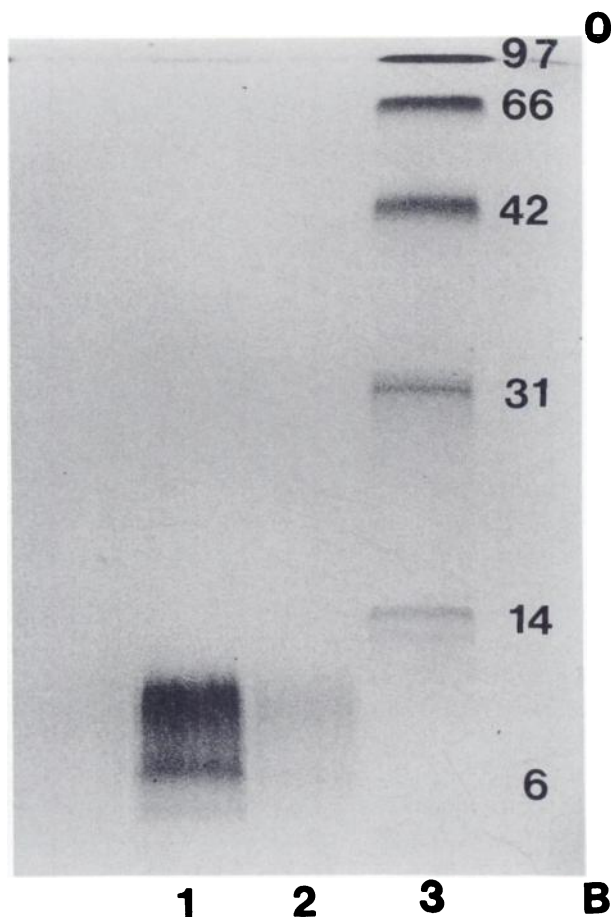


**FIGURE 7**  
 SDS-PAGE (under reduction conditions) of  $^{111}\text{In}$ -SCN-Bz-DTPA-NP-4 IgG in tissue extracts 24 hr after injection: lane 1, liver extract (LMWF); lane 2, kidney extract (LMWF); lane 3, low molecular weight standards (Bio-Rad, Richmond, CA) MW  $\times 10^3$ , run on a 12% gel, stained with Coomassie blue. Origin = O; Bottom = B.

the kidney, since in the urine (lanes 3 and 9) all the activity is associated with only one band at the bottom of the gel. In the liver and kidney extracts of the control group (lanes 5 and 7), 100% of the activity migrated to the bottom of the gel, similar to the  $^{111}\text{In}$ -SCN-Bz-DTPA (lane 1).

#### HPIEC Analysis

Most of the LMWF activity (84%) was eluted in the first 36 sec, similar to  $^{111}\text{In}$ -SCN-Bz-DTPA control (Fig. 8), and the remainder of the radioactivity eluted in 1 to 5 min.

#### Thin-Layer Chromatography Analysis

Table 1 shows the results of ITLC and silica gel (SG) chromatography. The majority of the activity migrates to the solvent front (SF), as in the  $^{111}\text{In}$ -DTPA control. This result further indicates that  $^{111}\text{In}$  radioactivity recovered from the tissues in the LMWF is associated with DTPA and a small fraction (5%–12%) remains at the origin, possibly as precipitated amino acids or peptide fragments (ninhydrin-positive).

#### DISCUSSION

The major limitation of MABs labeled with radiometals, particularly  $^{111}\text{In}$  and gallium-67, has been accretion of radioactivity in the liver (12), and with MAB fragments' accretion in the kidney (23). Increased bone uptake, as in the case of  $^{90}\text{Y}$ -labeled-MAB (13,24,25), would lead to bone marrow toxicity and may limit the usefulness of metal-labeled MABs for radioimmunotherapy of cancer. Chelates that could bind these radiometals more tightly, thus preventing exchange of the radiometal with serum proteins, particularly transferrin

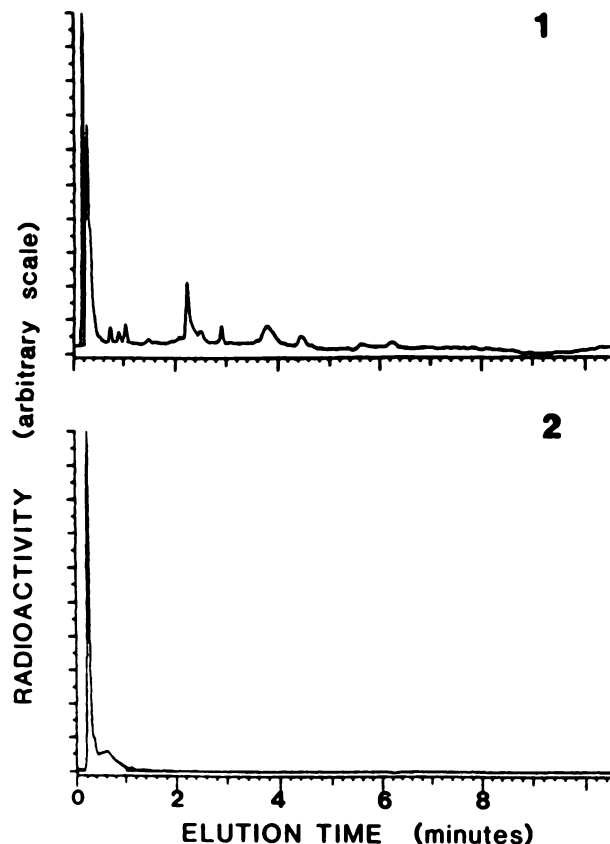


**FIGURE 8**  
HPLC analysis of 1:  $^{111}\text{In}$ -SCN-Bz-DTPA-NP-4 IgG liver extract (LMWF) and 2:  $^{111}\text{In}$ -SCN-Bz-DTPA control. Gradient: 0–5 min 0–100% buffer B; 1 min hold at 100% B; 6–11 min 0% buffer B. Flow: 1.0 ml/min.

**TABLE 1**  
Thin-layer Chromatography Analysis of Radioactivity in Tissue Extracts, Urine, and Plasma\*

Sample	TLC-SG Methanol:c. ammonia (4:1) pH 10.0		ITLC-SG Methanol:1% citrate (1:1) pH 4.0	
	Rf	% applied activity	Rf	% applied activity
Liver (LMWF)	0.16	12.0%	0.16	10.0%
	0.51	9.0%	0.60	7.0%
Kidney (LMWF)	1.00	72.0%	0.84	75.0%
	0.16	5.2%	0.16	6.0%
Urine	0.58	15.0%	0.60	12.0%
	1.00	74.0%	1.00	78.0%
Plasma DTPA	0.16	5.5%	0.20	0.8%
	1.00	94.0%	1.00	99.0%
DTPA	0.16	98.0%	0.20	99.0%
	0.10	0.1%	0.10	0.1%
	1.00	99.0%	1.00	99.0%

\* One day after injection of  $^{111}\text{In}$ -SCN-Bz-DTPA-NP-4 IgG or  $^{111}\text{In}$ -SCN-Bz-DTPA.

(26), and in some cases serum albumin (27), are desirable, but the labeled antibody would still be catabolized by many tissues and the isotope would be either eliminated or retained in the target tissue. Thus, an investigation of the products formed during the metabolism of radiometal-labeled IgG or  $\text{F}(\text{ab}')_2$  represents a first stage in developing an understanding of the problems or prospects for a MAb radioconjugate.

The *in vivo* stability of the radiolabeled antibody in the plasma is a principal concern. Cole et al. (27) studied the plasma stability of a number of chelates *in vitro*. Although this is a good preliminary screening method when examining a large number of new chelates, *in vivo* studies incorporate an investigation of the plasma stability with additional information concerning the processing that may occur as the products circulate through tissues. Size-exclusion HPLC was used to analyze the stability of the labeled MAb both in plasma and in tissues. This is of particular importance if the presence of  $^{111}\text{In}$  transchelated to ferritin or transferrin is suspected, because unlike ITLC, the molecular size of the products could be assessed by HPLC.

Size-exclusion HPLC of the plasma taken from animals between one and four days did not reveal any significant products other than intact IgG or  $\text{F}(\text{ab}')_2$  that had retained their immunoreactivity. Thus, within the sensitivity of the method used, there was no detectable exchange of  $^{111}\text{In}$  with other metal-binding serum proteins. However, these results would also suggest that we were unable to measure any significant level of radioactivity that may represent material metabolized in the tissues that was in transit in the serum. Indeed, even the HPLC profiles of the radioactivity in the perfused fluids from the liver and kidneys were identical to the radioactivity in the plasma. Since a significant portion of the radioactivity in the tissue extracts was a LMWF, it is likely that the perfusion only removed radioactivity localized in the blood vessels and that the LMWF was either in the cells or the interstitial space of the tissue.

In contrast to the plasma, radioactivity in tissue extracts was characterized by two distinct peaks, one was native-sized IgG or  $\text{F}(\text{ab}')_2$ , and the other a LMWF. The buffers used in these studies were formulated to reduce the possibility that enzymatic degradation of the immunoglobulin would occur, and controls for the extraction process were included to ensure that the extracted material was representative of the radioactivity *in situ*. Thus, we believe that these products represent the catabolic breakdown in the tissues and were not due to our experimental procedure.

The results from these studies suggest that the intact IgG or  $\text{F}(\text{ab}')_2$  is converted to the LMWF directly without any intervening metabolic products. Furthermore, the rate of catabolism was similar in the liver and kidney. Several investigators have studied radiolabeled

antibody metabolism. Shochat et al. (28) investigated the metabolism of radioiodinated or indium-labeled antibodies derivatized with cyclic-DTPA anhydride in hamsters bearing the same human tumor xenograft, and concluded that the majority of the  $^{111}\text{In}$  is retained in the liver as a small molecular weight moiety. Mathias and Welch (29) studied the metabolism in the rat of radioiodinated and indium-labeled MAb entrapped in liposomes, and suggested that the mechanism of liver retention of this metal is due to translocation of the indium from DTPA to some intracellular binding sites, but unfortunately their communication does not mention the kind of chelate used. We did not find evidence of  $^{111}\text{In}$  transfer to transferrin either in plasma or in liver tissue. Indeed, reduced transchelation has been reported for antibodies with a Bz-DTPA versus a DTPA group (30).

An important aspect of MAb-targeted therapy is whether the MAb with its cytotoxic agent is internalized. Although not conclusively shown in this study, but nevertheless an intriguing speculation, is that the LMWF radioactivity was located intracellularly in the tissue. Biodistribution studies with this MAb conjugate have shown a very slow rate of clearance of radioactivity in the tissues over the time course of this study (18), yet during this same period, the proportion of native-sized immunoglobulin in the tissues is declining rapidly with an increasing proportion of the LMWF. Characterization of the LMWF revealed a molecular size between 2,000 and 3,000 daltons. It seems unlikely that such a small component would be held in the interstitial space of the tissues or bound to cell membranes, but rather that is sequestered within the cells. In this case, the immunoglobulin may have been metabolized intracellularly and the metabolic product (the LMWF) could not escape, or the immunoglobulin may have been metabolized extracellularly, and the LMWF was then internalized and sequestered. Recently, Ward et al. (31) reported that the administration of chelating agents, such as desferrioxamine and DTPA, were not effective in reducing the high background tissue radioactivity in patients undergoing scanning with  $^{111}\text{In}$ -labeled MAb, suggesting that label fixed in the tissues was inaccessible to the chelating agents. Goodwin et al. (32) have shown that early administration of a flushing dose of non-radioactive In-Bz-DTPA decreased whole body radioactivity, but that following the rapid response to flushing, the activity remaining in the body decayed at about the same rate as the initial activity prior to flushing. These results suggest that following internalization and metabolism of the MAb, any radiolabel released from the antibody and fixed in the tissue is unavailable for binding by the chelator. Hershko (33) reported that DTPA was unable to remove metal ions from tissues because it is charged and would not pass through cell membranes. Thus, if the labeled MAbs pass into the

cells and the  $^{111}\text{In}$ -DTPA is metabolized from the MAb, it may be unable to pass through the cell membrane and would remain trapped in the cell for prolonged periods. Clarification of the cellular location of the radionuclide requires further investigation, but the implications of these data may have significant impact on the use of various radionuclides or drugs that require internalization for an optimal antitumor effect.

Our HPIEC analysis of the LMWF in liver extracts shows a small amount of radioactivity (16%) that binds to the resin, possibly as an  $^{111}\text{In}$ -peptide, and the majority of the unbound activity chelated to DTPA. We did not include a series of  $^{111}\text{In}$ -Bz-DTPA-peptide fragments as a control in this study, but it appears from our  $^{111}\text{In}$ -SCN-Bz-DTPA control study that  $^{111}\text{In}$ -SCN-Bz-DTPA does not bind to the anion exchange resin used, and this further supports our assumption that a large part of the radioactivity found in liver tissue should be bound to DTPA. Because this anion exchange cartridge offers superior separation of small peptides, the radioactivity was found associated with several peaks. In contrast, the SDS-PAGE analysis showed two major metabolites besides the  $^{111}\text{In}$ -SCN-Bz-DTPA band. Reduced liver levels of  $^{111}\text{In}$  with antibodies conjugated with SCN-Bz-DTPA (10), over those conjugated with the cyclic anhydride of DTPA, was explained by Hnatowich (34) as increased instability of the thiourea bond in the SCN-Bz-DTPA, versus the acid amide formed by the anhydride with protein amines. Whether the presence of the indium-labeled chelate in liver, kidney and urine is due to metabolic breakdown of the labeled IgG in the tissues, or to instability of the thiourea bond whereby this chelator is conjugated to MAb, has not been demonstrated. Shochat et al. (28) reported a LMWF in liver tissue extract of animals injected with  $^{111}\text{In}$ -labeled MAb linked to the cyclic anhydride of DTPA.

In our view, the increase of the LMWF in normal tissue and tumor, as a function of time, indicates a breakdown of the labeled IgG and  $\text{F(ab')}_2$  in the tissues rather than an instability of the Bz-DTPA chelator. All this evidence suggests that the difference between the liver retention of MAb may be due to differences in the rate of catabolism of the MAb when modified by different linkage chemistry.

In addition to the liver, the kidney may play a major role in the catabolism of plasma proteins, especially antibody fragments (35,36). This would be due to the passage of the fragments through the glomerular filtrate, and exposure to catabolic sites in the renal tubules (37). In comparing the molecular form of the radioactivity in the urine to that found in the extracts of the kidney by SDS-PAGE, we found for IgG as well as for the  $\text{F(ab')}_2$  (Fig. 6, lanes 6 and 9) that there are two distinct low molecular weight bands. In the urine (Fig. 6, lanes 3 and 9), there is principally one band present, suggest-

ing that some of the metabolites are further processed in the kidney and excreted in the urine, mainly as one LMW component.

The results in the urine are similar when analyzed by HPLC. Our findings, and the findings reported by Adams et al. (38), show that  $^{111}\text{In}$  in the urine is present still bound to the Bz-DTPA chelator. Our data suggest that the MAb has been degraded to short  $^{111}\text{In}$ -SCN-Bz-DTPA-peptide fragments and  $^{111}\text{In}$ -SCN-Bz-DTPA. Nevertheless, we cannot exclude the possibility that some of the indium present in the tissues was in the form of colloidal indium, and that this material was not recovered from the HPLC column.

In order to perform these studies, animals were injected with 1 to 5 mCi (37 to 185 MBq) (0.33 to 1.0 mg MAb protein). Protein dose has been reported to influence the biodistribution of radiometal-labeled MAbs (38,39), but its influence on the catabolism of the labeled MAb has not been addressed. Since biodistribution studies in animals are more frequently conducted with significantly less MAb, we cannot be certain that the metabolic products defined in this study are similar to those that may be seen when less protein is injected. Due to the limitations with respect to the specific activity of the  $^{111}\text{In}$ -labeled MAb, this issue could not be resolved. Nevertheless, a recent publication (40) regarding biodistribution studies in hamsters with GW-39 human colon tumors and injected with large doses of MAb shows that the percentage injected dose per gram (ID/g) of the antibody bound per gram of blood and to normal tissues, including liver and kidney, remained constant (within statistical variations) across the dose range of 0.05 to 2.0 mg antibody. If the percentage of indium in normal tissues is fairly constant over a wide range of protein doses, this may also be reflected in the metabolic products.

In conclusion, the elucidation of the metabolic products of the  $^{111}\text{In}$ -DTPA-MAb conjugates may provide insights and approaches that would reduce the undesirable deposition of MAbs conjugated with metallic radionuclides. Other isotopes used to label MAbs, such as  $^{90}\text{Y}$ , rhenium-186, or copper-67, which are metabolized differently than  $^{111}\text{In}$ , may also be worthy of evaluation by this approach.

#### ACKNOWLEDGMENTS

The authors thank Drs. K. Chang and G. Griffiths (Immunomedics Inc, Newark, NJ) and Dr. Y.Y. Tu (CMMI, Newark, NJ) for helpful discussions, and Mrs. R. Aninipot for technical assistance.

This work was supported in part by USPHS grant CA39841 from the NIH. It was also presented in part at the Society of Nuclear Medicine's 36th Annual Meeting in St. Louis, MO, 1989.

#### REFERENCES

1. Goldenberg DM. Targeting of cancer with radiolabeled antibodies: Prospects for imaging and therapy. *Arch Pathol Lab Med* 1988; 112:580-587.
2. Brady LW, Woo DV, Hendel ND, Markoe AM, Koprowski H. Therapeutic and diagnostic uses of modified monoclonal antibodies. *Int J Radiat Oncol Biol Physics* 1987; 3:1535-1544.
3. Dillman RO, Royston I. Applications of monoclonal antibodies in cancer therapy. *Br Med Bull* 1984; 40:240-246.
4. Hnatowich DJ, Childs RL, Lanteigne D. The preparation of DTPA-coupled antibodies radiolabeled with metallic radionuclides: an improved method. *J Immunol Methods* 1983; 65:147-157.
5. Rainsbury RM, Westwood JH, Coombes RC, et al. Location of metastatic breast carcinoma by a monoclonal antibody chelate labeled with indium-111. *Lancet* 1983; 2:934-938.
6. Meares CF. Chelating agents for the binding of metal ions to antibodies. *Int J Nucl Med Biol* 1986; 13:311-318.
7. Sundberg MW, Meares CF, Goodwin DA, Diamanti CI. Selective binding of metal ions to macromolecules using bifunctional analogs of EDTA. *J Med Chem* 1974; 17:1304-1307.
8. Eckelman WC, Paik CH, Reba R. Radiolabeling of antibodies. *Cancer Res* 1980; 40:3036-3042.
9. Krejcarek GE, Tucker KL. Covalent attachment of chelating groups to macromolecules. *Biochem Biophys Res Commun* 1977; 77:581-585.
10. Esteban JM, Schlom J, Gansow OA, et al. New method the chelation of  $^{111}\text{In}$  to monoclonal antibodies: biodistribution and imaging of athymic mice bearing human colonic carcinomas xenografts. *J Nucl Med* 1987; 28:861-870.
11. Hnatowich DJ, Chinol M, Siebecker DA, et al. Patient distribution of intraperitoneally administered yttrium-90-labeled antibody. *J Nucl Med* 1988; 29:1428-1434.
12. Perkins AC, Pimm MV. Differences in tumor and normal tissue concentration of iodine and indium labeled monoclonal antibody. I: The effect on image contrast in clinical studies. *Eur J Nucl Med* 1985; 11:295-299.
13. Sharkey RM, Motta-Hennessy C, Gansow OA, et al. Biodistribution and radiation dose estimates for yttrium- and iodine-labeled monoclonal antibody IgG and fragments in nude mice bearing human colonic tumor xenografts. *Cancer Res* 1990; 50:2330-2336.
14. Brechbiel MW, Gansow OA, Atcher RW, et al. Synthesis of 1-(p-isothiocyanatobenzyl) derivatives of DTPA and EDTA. Antibody labeling and tumor-imaging studies. *Inorg Chem* 1986; 25:2772-2781.
15. Alvarez V, Wen ML, Lee C, Lopes D, Rodwell JD, McKearn TJ. Site-specifically modified  $^{111}\text{In}$  labeled antibodies give low liver background and improved radioimmunoscintigraphy. *Int J Nucl Med Biol* 1986; 13:347-352.
16. Haseman MK, Goodwin DA, Meares CF, et al. Metabolizable  $^{111}\text{In}$  chelate conjugated anti-idiotypic monoclonal antibody for radioimmunodetection of lymphoma in mice. *Eur J Nucl Med* 1986; 12:455-460.
17. Blend MJ, Greager JA, Atcher RW, et al. Improved sarcoma imaging and reduced hepatic activity with indium-111-SCN-Bz-DTPA linked to MoAb 19024. *J Nucl Med* 1988; 29:1810-1816.
18. Sharkey RM, Motta-Hennessy C, Gansow OA, Brechbiel M, Fand I, Goldenberg DM. Selection of a DTPA chelate conjugate for monoclonal antibody targeting to a human colonic tumor in mice. *Int J Cancer* 1990; in press.
19. Primus JF, Newell K, Blue A, Goldenberg DM. Immunological heterogeneity of carcinoembryonic antigen: antigenic de-

- terminants of carcinoembryonic antigen distinguished by monoclonal antibodies. *Cancer Res* 1983; 43:688-692.
20. Sharkey RM, Kaltovich F, Shih LB, Fand I, Govelitz G, Goldenberg DM. Radioimmunotherapy of human colonic cancer xenografts with <sup>90</sup>Y-labeled monoclonal antibodies to carcinoembryonic antigen. *Cancer Res* 1988; 48:3270-3275.
  21. Tu YY, Primus JF, Shochat D, Goldenberg DM. Purification and characterization of carcinoembryonic antigen from GW-39, a xenografted human colonic tumor system. *Tumor Biol* 1988; 9:212-220.
  22. Goldenberg DM, Witte S, Elster K. GW-39: A new human tumor serially transplantable in the golden hamster. *Transplantation* 1966; 4:760-763.
  23. Otsuka FL, Fleishman JB. Comparative studies using <sup>125</sup>I and <sup>111</sup>In-labeled monoclonal antibodies. *Eur J Nucl Med* 1986; 11:295-299.
  24. Anderson WT, Squire RA, Strand M. Specific radioimmunotherapy using <sup>90</sup>Y-labeled monoclonal antibody in erythroleukemic mice. *Cancer Res* 1987; 47:1905-1912.
  25. Stewart JSW, Hird V, Snook D, Sullivan M, Myers MJ, Epenetos AA. Intraperitoneal <sup>131</sup>I and <sup>90</sup>Y labeled monoclonal antibodies for ovarian cancer: pharmacokinetics and normal tissue dosimetry. *Int J Cancer* 1988; (suppl. 3):71-76.
  26. Hnatowich D. Label stability in serum of four radionuclides on DTPA-coupled antibodies. An evaluation. *Int J Nucl Med Biol* 1986; 13:353-358.
  27. Cole WA, DeNardo SJ, Meares CF, et al. Serum stability of <sup>67</sup>Cu chelates: comparison with <sup>111</sup>In and <sup>57</sup>Co. *Int J Nucl Med Biol* 1986; 13:363-368.
  28. Shochat D, Sharkey RM, Vattay A, Primus FJ, Goldenberg DM. In-111 chelated by DTPA-antibody is retained in the liver as a small molecular weight moiety [Abstract]. *J Nucl Med* 1986; 27:943.
  29. Mathias CJ, Welch MJ. Studies on the entrapment of <sup>111</sup>In in the liver following administration of proteins labeled using bifunctional chelates [Abstract]. *J Nucl Med* 1987; 28:657-658.
  30. Goodwin DA, Meares CF, McTigue M. Metal decomposition rates of <sup>111</sup>In-DTPA and EDTA conjugates of monoclonal antibodies *in vivo*. *Nucl Med Comm* 1986; 7:831-838.
  31. Ward MC, Roberts KR, Westwood JH, Coombes RC, McCready VR. The effect of chelating agents on the distribution of monoclonal antibodies in mice. *J Nucl Med* 1986; 27:1746-1750.
  32. Goodwin DA, Meares CF, David GF, et al. Monoclonal antibodies as reversible equilibrium carriers of radiopharmaceuticals. *Int J Nucl Med Biol* 1986; 13:383-391.
  33. Hershko C. A study of the chelating agent diethylenetriamine pentaacetic acid using selective radioiron probes of reticulo-endothelial and parenchymal iron stores. *J Lab Clin Med* 1975; 85:913-921.
  34. Hnatowich DJ. On the accumulation in liver of indium-111 following administration of the B72.3 antibody. *J Nucl Med* 1989; 30:1575-1576.
  35. Waldman TA, Strober W. Metabolism of immunoglobulins. *Prog Allergy* 1969; 13:1-110.
  36. Wochner RD, Strober RD, Waldman TA. The role of the kidney in the catabolism of Bence Jones proteins and immunoglobulin fragments. *J Exp Med* 1967; 126:207-221.
  37. Arend WP, Silverblatt FJ. Serum disappearance and catabolism of homologous immunoglobulin fragments in rats. *Clin Exp Immunol* 1975; 22:502-513.
  38. Adams GP, DeNardo SJ, Shrikant VD, et al. Effect of mass of <sup>111</sup>In-Bz-EDTA monoclonal antibody on hepatic uptake and processing in mice. *Cancer Res* 1989; 49:1707-1711.
  39. Otsuka FL, Welch MJ. Evidence of a saturable clearance mechanism for <sup>111</sup>In-labeled clearance mechanism for <sup>111</sup>In-labeled monoclonal antibodies. *Int J Nucl Med Biol* 1985; 12:331-332.
  40. Fenwick G, Philpott GW, Connett JM. Biodistribution and histological localization of anti-human colon cancer monoclonal antibody (MAb) 1A3: The influence of administered MAb dose on tumor uptake. *Int J Cancer* 1989; 44:1017-1027.